Frontiers of Information Technology & Electronic Engineering
www.jzus.zju.edu.cn; engineering.cae.cn; www.springerlink.com
ISSN 2095-9184 (print); ISSN 2095-9230 (online)
E-mail: jzus@zju.edu.cn

Event-based H_∞ control for piecewise-affine systems subject to actuator saturation*

Yonghao JIANG†, Wei WU†‡, Xuyang LOU†‡, Zhengxian JIANG, Baotong CUI

MOE Key Laboratory of Advanced Process Control for Light Industry, Jiangnan University, Wuxi 214122, China

†E-mail: y.h.jiang@foxmail.com; weiwu@jiangnan.edu.cn; Louxy@jiangnan.edu.cn

Received Nov. 6, 2019; Revision accepted June 9, 2020; Crosschecked Nov. 16, 2020; Published online Jan. 8, 2021

Abstract: We deal with event-triggered H_∞ controller design for discrete-time piecewise-affine systems subject to actuator saturation. By considering saturation information, a novel event-triggered strategy is proposed to conserve communication resources. A linear matrix inequality based condition is derived based on a piecewise Lyapunov function. This condition guarantees the stability of the closed-loop system with a certain H_∞ performance index and reduces the number of transmitted signals. Numerical examples are given to show the efficiency of our method.

Key words: Event-triggered control; Piecewise-affine system; Linear matrix inequality; Actuator saturation; H_∞ performance

https://doi.org/10.1631/FITEE.1900601 **CLC number:** TP273

1 Introduction

Networked control systems (NCSs) have drawn considerable attention because of their advantages in terms of cost, flexibility, and maintainability (Postoyan et al., 2015). In NCSs, the measured outputs and/or actuator signals are transmitted through a shared communication network. However, in practical situations, some problems, such as network congestion in shared networks and high energy consumption of wireless devices, exist. To overcome these obstacles, control systems based on aperiodic sampling strategies, particularly event-triggered control, have been proposed (Hespanha et al., 2007). Unlike traditional periodic time-triggered control strategies in which signals are transmitted at fixed time, the event-triggered control (ETC) scheme is based on an event generated by some well-designed event-triggering conditions. This scheme can reduce signal transmission while maintaining a satisfactory closed-loop performance (Åarzén, 1999; Åström and Bernhardsson, 1999; Tabuada, 2007; Liu JL et al., 2020b).

Most event-triggered techniques, however, deal with continuous systems, in which the plant state/output is monitored continuously, and therefore special hardware is required. Moreover, the treatment of Zeno behavior (Lei et al., 2018) poses a fundamental problem. To address these issues, periodic ETC (PETC) was proposed (Heemels et al., 2013), in which the event-triggering condition was verified only at some given sampling instants. Hence, the minimum inter-event time is naturally guaranteed by the sampling interval, and therefore Zeno behavior is prevented. Based on the PETC scheme, security distributed state estimation for nonlinear networked systems against denial-of-service attacks was proposed (Liu JL et al., 2020c), and secure leader-following consensus control was examined for multi-agent systems considering multiple cyber attacks (Liu JL et al., 2020a). In addition, some discrete-time strategies, which are essentially PETC

‡ Corresponding authors

* Project supported by the National Natural Science Foundation of China (No. 61807016), the China Postdoctoral Science Foundation (No. 2018M642160), the Jiangsu Province Postdoctoral Fund of China (No. 1701095B), and the Natural Science Foundation of Jiangsu Province, China (No. BK20201340)

ORCID: Yonghao JIANG, https://orcid.org/0000-0002-4772-0115; Wei WU, https://orcid.org/0000-0001-8283-0654; Xuyang LOU, https://orcid.org/0000-0002-7499-1308

© Zhejiang University Press 2021

approaches, were proposed (Eqtami et al., 2010; Wu et al., 2015, 2016; Aranda-Escolástico et al., 2017). The PETC strategy is easily implementable since it can be implemented in a standard time-sliced embedded software architecture. However, many important results with regard to the aforementioned ETC design problem were developed for linear time-invariant (LTI) systems and nonlinear systems; few studies examined piecewise-affine (PWA) systems.

PWA systems are an important class of hybrid systems with wide applications. Many chaotic systems can be described as PWA systems (Saito et al., 1995). Moreover, many nonlinear systems can be approximated by PWA systems; thus, PWA systems provide a powerful tool for the analysis and synthesis of nonlinear control systems (Heemels et al., 2001). In fact, PWA systems can be used to analyze smooth nonlinear systems with an arbitrary accuracy (Sontag, 1981). In Qiu et al. (2018), the delay-dependent robust and reliable H_∞ static output feedback control problem for uncertain discrete-time PWA systems with time-varying delays and actuator faults was discussed. The H_∞ static output feedback control problem for PWA systems with actuator faults was examined (Qiu et al., 2017). Furthermore, H_∞ robust model predictive control was proposed for constrained PWA systems (Esfahani and Pieper, 2017). Event-triggered fault detection control for PWA systems was investigated by Liu Y et al. (2017). A quadratic cost function was considered for control performance to obtain an optimized event-triggering controller for discrete-time PWA systems by minimizing the cost function (Ma et al., 2018).

Meanwhile, it is well known that most practical systems suffer from actuator saturation because of the natural physical limitations of actuators. In this sense, state feedback control under an event-triggering condition for LTI systems was proposed to maximize the estimate of the domain of attraction (Wu et al., 2014). Another method (Zuo et al., 2016) was proposed to handle the saturation nonlinearity by transforming the saturation problem into dead zone nonlinearity with the generalized sector condition (Tarbouriech et al., 2011). Li et al. (2018) investigated the problem of event-triggered dynamic output feedback control for continuous-time linear systems in the presence of actuator saturation. Regarding PWA systems, an event-triggered controller for PWA systems subject to input saturation was investigated by Ma et al. (2019); however, robustness was not discussed. The robustness and l_2-gain control problem for uncertain PWA systems with actuator saturation was addressed by Chen YG et al. (2014). A robust H_∞ controller was developed by Gao et al. (2009) for constrained uncertain PWA systems.

In this study, the event-triggered H_∞ control problem is examined for PWA systems subject to actuator saturation. The piecewise quadratic Lyapunov function is employed. For controllers, a set of linear matrix inequalities (LMIs) are solved.

The main contributions of this paper can be highlighted as follows: (1) An event-triggered H_∞ control problem is investigated for the first time for PWA systems subject to actuator saturation. (2) A novel event-triggered strategy is proposed by considering actuator saturation. Compared with strategies without saturation information, our method can reduce data transmission when saturation occurs. (3) Optimization approaches are provided to optimize the H_∞ performance and the domain of attraction. We provide several numerical examples to illustrate the effectiveness and advantages of the proposed approach.

Notations are described as follows: $\|\boldsymbol{x}\| = \sqrt{\boldsymbol{x}^{\mathrm{T}}\boldsymbol{x}}$ denotes the Euclidean norm. $|\cdot|$ denotes the absolute value. $l_2[0,\infty)$ stands for the space of square summable infinite vector sequences over $[0,\infty)$. $\boldsymbol{P}^{\mathrm{T}}$ and $\boldsymbol{P}^{-1}$ represent the transpose and the inverse of matrix $\boldsymbol{P}$, respectively. $\boldsymbol{I}$ and $\boldsymbol{0}$ are the identity matrix and zero matrix with compatible dimensions, respectively. Matrix $\left(\begin{smallmatrix}\boldsymbol{A} & *\\ \boldsymbol{B} & \boldsymbol{C}\end{smallmatrix}\right)$ is a symmetric matrix of $\left(\begin{smallmatrix}\boldsymbol{A} & \boldsymbol{B}^{\mathrm{T}}\\ \boldsymbol{B} & \boldsymbol{C}\end{smallmatrix}\right)$. For a symmetric matrix $\boldsymbol{P}\in\mathbb{R}^{n\times n}$, $\boldsymbol{P}>0$ ($\boldsymbol{P}\geq 0$) means that $\boldsymbol{P}$ is positive definite (semi-positive definite). $\mathrm{diag}(\boldsymbol{A},\boldsymbol{B})$ denotes a block diagonal matrix composed of blocks $\boldsymbol{A}$ and $\boldsymbol{B}$.

2 Problem formulation

Consider the discrete-time PWA system as

$$\begin{cases}\boldsymbol{x}(k+1)=\boldsymbol{A}_i\boldsymbol{x}(k)+\boldsymbol{B}_{1i}\mathrm{sat}(\boldsymbol{u}(k))+\boldsymbol{B}_{2i}\boldsymbol{\omega}(k)+\boldsymbol{a}_i,\\ \boldsymbol{z}(k)=\boldsymbol{C}_i\boldsymbol{x}(k)+\boldsymbol{D}_{1i}\mathrm{sat}(\boldsymbol{u}(k))+\boldsymbol{D}_{2i}\boldsymbol{\omega}(k),\end{cases}\tag{1}$$

where $\boldsymbol{x}(k)\in\boldsymbol{\chi}_i$, $i\in\mathcal{I}$, and $\boldsymbol{\chi}_i\subseteq\mathbb{R}^n$ denotes a partition of the state space into a number of closed

(possibly unbounded) polyhedral regions. We refer to each $\boldsymbol{\chi}_i$ as a cell. $\mathcal{I}$ is the index set of these polyhedral cells and is partitioned as $\mathcal{I}=\mathcal{I}_0\cup\mathcal{I}_1$, where $\mathcal{I}_0$ is the index set of cells containing the origin and $\mathcal{I}_1$ is the index set of cells not containing the origin. $\boldsymbol{x}(k)\in\mathbb{R}^n$ refers to the system state vector; $\boldsymbol{u}(k)\in\mathbb{R}^m$ is the control input; $\boldsymbol{z}(k)\in\mathbb{R}^p$ is the controlled output vector; $\boldsymbol{\omega}(k)\in\mathbb{R}^q$ is an energy bounded disturbance assumed to belong to $l_2[0,\infty)$, satisfying $\sum_{k=0}^{\infty}\boldsymbol{\omega}^{\mathrm{T}}(k)\boldsymbol{\omega}(k)\leq\omega_{\max}<\infty$; matrices $\boldsymbol{A}_i$, $\boldsymbol{B}_{1i}$, $\boldsymbol{B}_{2i}$, $\boldsymbol{C}_i$, $\boldsymbol{D}_{1i}$, $\boldsymbol{D}_{2i}$ represent the known real constant matrices of the i^{th} local model with appropriate dimensions; constant vector $\boldsymbol{a}_i$ denotes the offset term. The saturated input can be expressed as $\mathrm{sat}(\boldsymbol{u})=(\mathrm{sat}(\boldsymbol{u}_{(1)}),\ \mathrm{sat}(\boldsymbol{u}_{(2)}),\ \ldots,\ \mathrm{sat}(\boldsymbol{u}_{(m)}))^{\mathrm{T}}$, where $\mathrm{sat}(\boldsymbol{u}_{(l)})=\mathrm{sgn}(\boldsymbol{u}_{(l)})\min\{|\boldsymbol{u}_{(l)}|,\ \boldsymbol{u}_{0(l)}\}$ $(l=1,2,\cdots,m)$ with a saturation level $\boldsymbol{u}_0$.

As a special case of $\boldsymbol{\chi}_i$ $(i\in\mathcal{I}_0)$, system (1) becomes the so-called piecewise linear (PWL) model:

$$\begin{cases}\boldsymbol{x}(k+1)=\boldsymbol{A}_i\boldsymbol{x}(k)+\boldsymbol{B}_{1i}\mathrm{sat}(\boldsymbol{u}(k))+\boldsymbol{B}_{2i}\boldsymbol{\omega}(k),\\ \boldsymbol{z}(k)=\boldsymbol{C}_i\boldsymbol{x}(k)+\boldsymbol{D}_{1i}\mathrm{sat}(\boldsymbol{u}(k))+\boldsymbol{D}_{2i}\boldsymbol{\omega}(k),\end{cases}$$

where $\boldsymbol{x}(k)\in\boldsymbol{\chi}_i$ $(i\in\mathcal{I}_0)$.

A partition of the state space can be achieved using the closed polyhedral cells $\boldsymbol{\chi}_i=\{\boldsymbol{x}\mid\boldsymbol{L}_i\boldsymbol{x}+\boldsymbol{l}_i\geq 0\}_{i\in\mathcal{I}}\in\mathbb{R}^n$, with $\boldsymbol{L}_i\in\mathbb{R}^{n\times n}$ and $\boldsymbol{l}_i\in\mathbb{R}^n$. Each polyhedral cell can be outer-approximated by a degenerate ellipsoid $\boldsymbol{\varepsilon}_i$. For the convenience of establishing LMI-based conditions, we adopt the ellipsoidal approximation instead of the polytopic description to describe the cells, since the former requires fewer parameters and can easily cast the synthesis problem as an optimization program involving a set of LMIs analytically parameterized by a vector. To describe the ellipsoid, assume that there exist matrices $\boldsymbol{E}_i\in\mathbb{R}^{m\times n}$ and $\boldsymbol{f}_i\in\mathbb{R}^m$ such that the polyhedral cells $\boldsymbol{\chi}_i$ $(i\in\mathcal{I})$ are included in the ellipsoidal regions $\boldsymbol{\varepsilon}_i$ $(i\in\mathcal{I})$, that is, $\boldsymbol{\chi}_i\subseteq\boldsymbol{\varepsilon}_i$ $(i\in\mathcal{I})$.

$$\boldsymbol{\varepsilon}_i=\{\boldsymbol{x}\mid\|\boldsymbol{E}_i\boldsymbol{x}+\boldsymbol{f}_i\|\leq 1\},\ i\in\mathcal{I}. \tag{2}$$

When the polyhedral cells $\boldsymbol{\chi}_i$ $(i\in\mathcal{I})$ have the following form:

$$\boldsymbol{\chi}_i=\{\boldsymbol{x}\mid d_1<\boldsymbol{c}_i^{\mathrm{T}}\boldsymbol{x}<d_2\},\ i\in\mathcal{I}, \tag{3}$$

the degenerate ellipsoid is described by $\boldsymbol{E}_i=2\boldsymbol{c}_i^{\mathrm{T}}/(d_2-d_1)$ and $f_i=-(d_2+d_1)/(d_2-d_1)$ (Rodrigues and Boyd, 2005; Rodrigues and Boukas, 2006).

Let $\Omega=\{(i,j)\mid\boldsymbol{x}(k)\in\boldsymbol{\chi}_i,\ \boldsymbol{x}(k{+}1)\in\boldsymbol{\chi}_j,\ i,j\in\mathcal{I}\}$ represent the index pairs denoting the possible switching of the state trajectories. Assume that when the state of the system shifts from region $\boldsymbol{\chi}_i$ to region $\boldsymbol{\chi}_j$ at instant k, the dynamics of the system is governed by the i^{th} local model.

Given the PWA system (1), we aim to design the state feedback controller as follows:

$$\boldsymbol{u}(k)=\boldsymbol{K}_i\boldsymbol{x}(k),\ i\in\mathcal{I}, \tag{4}$$

where $\boldsymbol{K}_i\in\mathbb{R}^{m\times n}$ $(i\in\mathcal{I})$ is the control gain to be designed later. When implemented in an event-triggering system, the communication between the controller and the actuator is no longer periodic, leading to the following state feedback control law:

$$\begin{cases}\hat{\boldsymbol{u}}(k)=\boldsymbol{K}_i\hat{\boldsymbol{x}}(k),\ i\in\mathcal{I},\\ \hat{\boldsymbol{u}}(0)=\boldsymbol{0},\end{cases} \tag{5}$$

where $\hat{\boldsymbol{u}}(k)$ is a signal defined as

$$\hat{\boldsymbol{u}}(k)=\begin{cases}\boldsymbol{u}(k), & \text{if event is triggered,}\\ \hat{\boldsymbol{u}}(k-1), & \text{otherwise.}\end{cases} \tag{6}$$

The control update policy can be obtained with an event generator, which will be discussed in Section 3.

The error function is defined as

$$\boldsymbol{e}(k)=\hat{\boldsymbol{u}}(k)-\boldsymbol{u}(k), \tag{7}$$

where $\hat{\boldsymbol{u}}(k)$ and $\boldsymbol{u}(k)$ refer to the control input signals updated at the last step and the current instant, respectively. When the event is triggered, the value of control input is held via a zero-order holder (ZOH) until the next event occurs. The structure of the event-based control loop considered in this study is shown in Fig. 1.

Definition 1 For convenience, define $\xi(\boldsymbol{P}_i,\rho)=\{\boldsymbol{x}\in\mathbb{R}^n|\boldsymbol{x}^{\mathrm{T}}\boldsymbol{P}_i\boldsymbol{x}\leq\rho\}$ and $\mathscr{L}(\boldsymbol{H}_i,\boldsymbol{u}_0)=\{\boldsymbol{x}\in\mathbb{R}^n|$

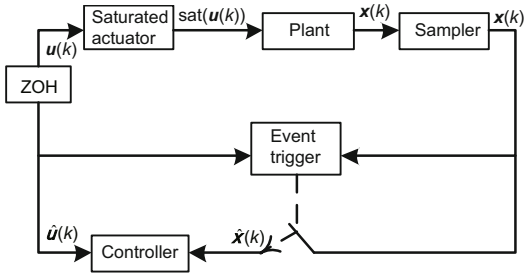


Fig. 1 Structure of the event-based control loop (ZOH: zero-order holder)

$|\boldsymbol{H}_{i(l)}\boldsymbol{x}| \leq \boldsymbol{u}_{0(l)}\}$ as a polyhedron, where matrix $\boldsymbol{P}_i > 0$ ($i \in \mathcal{I}$) is symmetric and positive definite, $\rho > 0$, and $\boldsymbol{H}_{i(l)}$ and $\boldsymbol{u}_{0(l)}$ are the l^{th} rows of $\boldsymbol{H}_{i(l)} \in \mathbb{R}^{m\times n}$ and $\boldsymbol{u}_0 \in \mathbb{R}^m$, respectively.

Lemma 1 (Hu et al., 2002) Let $\boldsymbol{u}, \boldsymbol{v} \in \mathbb{R}^m$. Suppose $|\boldsymbol{v}_{(l)}| < \boldsymbol{u}_{0(l)}$. Then, $\boldsymbol{u}$ and $\boldsymbol{v}$ are elements of the set defined as follows:

$$\text{sat}(\boldsymbol{u}) \in \text{co}\{\boldsymbol{\Lambda}_{is}\boldsymbol{u} + \boldsymbol{\Lambda}_{is}^{-}\boldsymbol{v} | s \in \{1, 2, \cdots, 2^m\}\},$$

where $\boldsymbol{\Lambda}_{is} \in \mathbb{R}^{m\times m}$ is a diagonal matrix whose elements are either 1 or 0, and $\boldsymbol{\Lambda}_{is}^{-} = \boldsymbol{I} - \boldsymbol{\Lambda}_{is}$. There are 2^m such matrices.

Corollary 1 Given an ellipsoid $\xi(\boldsymbol{P}_i, \rho)$ and a polyhedron $\mathscr{L}(\boldsymbol{H}_i, \boldsymbol{u}_0)$ if

$$\begin{pmatrix} \boldsymbol{P}_i & * \\ \boldsymbol{H}_{i(l)} & \boldsymbol{u}_{0(l)}^2/\rho \end{pmatrix} > 0, \tag{8}$$

then $\xi(\boldsymbol{P}_i, \rho) \subset \mathscr{L}(\boldsymbol{H}_i, \boldsymbol{u}_0)$.

Proof (Boyd and Vandenberghe, 2004) Suppose $\boldsymbol{x}(k) \in \mathscr{L}(\boldsymbol{H}_i, \boldsymbol{u}_0)$. Based on Lemma 1, the saturated control input can be expressed as

$$\begin{aligned} \text{sat}(\boldsymbol{u}(k)) = &\sum_{s=1}^{2^m} \eta_{is}(\boldsymbol{\Lambda}_{is}\boldsymbol{K}_i + \boldsymbol{\Lambda}_{is}^{-}\boldsymbol{H}_i)\boldsymbol{x}(k) \\ &+ \sum_{s=1}^{2^m} \eta_{is}\boldsymbol{\Lambda}_{is}\boldsymbol{e}(k), \end{aligned} \tag{9}$$

where $\eta_{is} \geq 0$ ($s = 1, 2, \ldots, 2^m$) and $\sum_{s=1}^{2^m} \eta_{is} = 1$.

By substituting Eq. (9) into Eq. (1), the closed-loop system can be described as

$$\begin{cases} \boldsymbol{x}(k+1) = \overline{\boldsymbol{A}}_i\boldsymbol{x}(k) + \overline{\boldsymbol{B}}_i\boldsymbol{e}(k) + \boldsymbol{B}_{2i}\boldsymbol{\omega}(k) + \boldsymbol{a}_i, \\ \boldsymbol{z}(k) = \overline{\boldsymbol{C}}_i\boldsymbol{x}(k) + \overline{\boldsymbol{D}}_i\boldsymbol{e}(k) + \boldsymbol{D}_{2i}\boldsymbol{\omega}(k), \end{cases} \tag{10}$$

where $\overline{\boldsymbol{A}}_i = \boldsymbol{A}_i + \sum_{s=1}^{2^m} \eta_{is}\boldsymbol{B}_{1i}(\boldsymbol{\Lambda}_{is}\boldsymbol{K}_i + \boldsymbol{\Lambda}_{is}^{-}\boldsymbol{H}_i)$, $\overline{\boldsymbol{B}}_i = \sum_{s=1}^{2^m} \eta_{is}\boldsymbol{B}_{1i}\boldsymbol{\Lambda}_{is}$, $\overline{\boldsymbol{C}}_i = \boldsymbol{C}_i + \sum_{s=1}^{2^m} \eta_{is}\boldsymbol{D}_{1i} \cdot (\boldsymbol{\Lambda}_{is}\boldsymbol{K}_i + \boldsymbol{\Lambda}_{is}^{-}\boldsymbol{H}_i)$, $\overline{\boldsymbol{D}}_i = \sum_{s=1}^{2^m} \eta_{is}\boldsymbol{D}_{1i}\boldsymbol{\Lambda}_{is}$, and $\boldsymbol{x}(k) \in \boldsymbol{\chi}_i$ ($i \in \mathcal{I}$).

Now, the control problem can be summarized as follows:

Problem 1 Considering the discrete-time PWA system (1) subject to actuator saturation, we design the state feedback controller (4) based on an event-triggering scheme, such that the closed-loop system is locally asymptotically stable with a guaranteed robust H_∞ performance index γ with respect to the energy bounded disturbance $\boldsymbol{\omega}(k)$. At the same time, the transmission between the plant and the controller is significantly reduced.

3 Main results

In this section, we will address the event-triggered H_∞ controller synthesis problem for PWA systems subject to actuator saturation. The event-triggering strategy is investigated to reduce signal transmission. Based on a piecewise Lyapunov function combined with some matrix inequality linearization procedures, the H_∞ state feedback controller (4) is designed with respect to the proposed event-triggering condition.

Now, consider the event generator as

$$\|\boldsymbol{e}(k)\| \geq \sigma\|\boldsymbol{K}_i\boldsymbol{x}(k)\|, \tag{11}$$

where $\sigma \in (0, 1)$ is a user-defined parameter. This event-triggering condition implies that when the error between the present sampled data $\boldsymbol{u}(k)$ and the latest triggered one $\hat{\boldsymbol{u}}(k)$ is not large enough, the control input of the system will not be transmitted until the condition is satisfied.

Remark 1 For set-point control, with the change of coordinates $\boldsymbol{x}(k) - \boldsymbol{x}_{\text{eq}}$ (Here, $\boldsymbol{x}_{\text{eq}}$ represents the equilibrium point), the problem can be transformed to the stabilization of the origin. In such a case, the event generator is adapted as

$$\|\boldsymbol{e}(k)\| \geq \sigma\|\boldsymbol{K}_i(\boldsymbol{x}(k) - \boldsymbol{x}_{\text{eq}})\|.$$

Based on the event generator (11), Eq. (6) can be written as

$$\hat{\boldsymbol{u}}(k) = \begin{cases} \boldsymbol{u}(k), & \|\boldsymbol{e}(k)\| \geq \sigma\|\boldsymbol{K}_i\boldsymbol{x}(k)\|, \\ \hat{\boldsymbol{u}}(k-1), & \|\boldsymbol{e}(k)\| < \sigma\|\boldsymbol{K}_i\boldsymbol{x}(k)\|. \end{cases} \tag{12}$$

Using the event generator designed above, it is easy to see that

$$\|\boldsymbol{e}(k)\| < \sigma\|\boldsymbol{K}_i\boldsymbol{x}(k)\| \tag{13}$$

always holds.

Since a saturated control input can be updated by another saturated one by applying event generator (12), to further reduce data transmission, Algorithm 1 is proposed (Suppose that the PWA system contains N subsystems).

Remark 2 In most event-triggered control approaches for systems with actuator saturation (Wu et al., 2014; Li et al., 2018; Ma et al., 2019), event-triggering strategies are based on state-based inequality conditions or control input based inequality conditions like inequality (11). However, saturation

Algorithm 1 Event-triggered and data transmission strategy

for $i=1:N$ **do**
  if $k=0$ **then**
    $\hat{\boldsymbol{u}}(0)=\boldsymbol{0}$
  else if $k=1$ **then**
    $\hat{\boldsymbol{u}}(k)=\boldsymbol{K}_i\boldsymbol{x}(k)$
  else
    if $\|\hat{\boldsymbol{u}}(k)-\boldsymbol{K}_i\boldsymbol{x}(k)\|\geq\sigma\|\boldsymbol{K}_i\boldsymbol{x}(k)\|$ **then**
      if $\|\hat{\boldsymbol{u}}(k-1)\|\geq\|\boldsymbol{u}_0\|$ && $\|\hat{\boldsymbol{u}}(k)\|\geq\|\boldsymbol{u}_0\|$ && $\hat{\boldsymbol{u}}(k-1)\hat{\boldsymbol{u}}(k)>0$ **then**
        $\hat{\boldsymbol{u}}(k)=\hat{\boldsymbol{u}}(k-1)$
      else
        $\hat{\boldsymbol{u}}(k)=\boldsymbol{K}_i\boldsymbol{x}(k)$
      end if
    else
      $\hat{\boldsymbol{u}}(k)=\hat{\boldsymbol{u}}(k-1)$
    end if
  end if
end for

is not taken into account, and therefore resources may be wasted when the actuator is saturated. Hence, in this study, a novel event-triggering strategy is developed by considering saturation.

For the closed-loop system (10), we employ a piecewise quadratic Lyapunov function in the following form:

$$V(k)=\boldsymbol{x}^{\mathrm{T}}(k)\boldsymbol{P}_i\boldsymbol{x}(k), \tag{14}$$

where $\boldsymbol{P}_i\in\mathbb{R}^{n\times n}$ is symmetric and positive definite.

The solution to Problem 1 is given below:

Theorem 1 For a given σ under the event-triggering condition (11), if there exist symmetric and positive definite matrices $\boldsymbol{Q}_i\in\mathbb{R}^{n\times n}$, $\boldsymbol{W}_i\in\mathbb{R}^{m\times n}$, and $\boldsymbol{G}_i\in\mathbb{R}^{m\times n}$, and parameters $\alpha_i>0$, $\beta_i>0$, and $\gamma>0$ $(i,j\in\mathcal{I},\,(i,j)\in\Omega)$, such that the following LMIs hold:

$$\begin{pmatrix}
\boldsymbol{Q}_i & * & * & * & * & * & * \\
\boldsymbol{0} & \alpha_i\boldsymbol{I} & * & * & * & * & * \\
\boldsymbol{0} & \boldsymbol{0} & \gamma^2\boldsymbol{I} & * & * & * & * \\
\boldsymbol{A}_i\boldsymbol{Q}_i+\boldsymbol{B}_{1i}\boldsymbol{\Theta}_i & \alpha_i\overline{\boldsymbol{B}}_i & \boldsymbol{B}_{2i} & \boldsymbol{Q}_j+\beta_i\boldsymbol{a}_i\boldsymbol{a}_i^{\mathrm{T}} & * & * & * \\
\boldsymbol{C}_i\boldsymbol{Q}_i+\boldsymbol{D}_{1i}\boldsymbol{\Theta}_i & \alpha_i\overline{\boldsymbol{D}}_i & \boldsymbol{D}_{2i} & \boldsymbol{0} & \boldsymbol{I} & * & * \\
\boldsymbol{W}_i & \boldsymbol{0} & \boldsymbol{0} & \boldsymbol{0} & \boldsymbol{0} & \frac{\alpha_i}{\sigma^2}\boldsymbol{I} & * \\
\boldsymbol{E}_i\boldsymbol{Q}_i & \boldsymbol{0} & \boldsymbol{0} & \beta_i\boldsymbol{f}_i\boldsymbol{a}_i^{\mathrm{T}} & \boldsymbol{0} & \boldsymbol{0} & \beta_i(\boldsymbol{f}_i\boldsymbol{f}_i^{\mathrm{T}}-\boldsymbol{I})
\end{pmatrix}$$
$$>0 \text{ for } i\in\mathcal{I}_1,\ i,j\in\mathcal{I},\ (i,j)\in\Omega, \tag{15a}$$

$$\begin{pmatrix}
\boldsymbol{Q}_i & * & * & * & * & * \\
\boldsymbol{0} & \alpha_i\boldsymbol{I} & * & * & * & * \\
\boldsymbol{0} & \boldsymbol{0} & \gamma^2\boldsymbol{I} & * & * & * \\
\boldsymbol{A}_i\boldsymbol{Q}_i+\boldsymbol{B}_{1i}\boldsymbol{\Theta}_i & \alpha_i\overline{\boldsymbol{B}}_i & \boldsymbol{B}_{2i} & \boldsymbol{Q}_j & * & * \\
\boldsymbol{C}_i\boldsymbol{Q}_i+\boldsymbol{D}_{1i}\boldsymbol{\Theta}_i & \alpha_i\overline{\boldsymbol{D}}_i & \boldsymbol{D}_{2i} & \boldsymbol{0} & \boldsymbol{I} & * \\
\boldsymbol{W}_i & \boldsymbol{0} & \boldsymbol{0} & \boldsymbol{0} & \boldsymbol{0} & \frac{\alpha_i}{\sigma^2}\boldsymbol{I}
\end{pmatrix}>0 \tag{15b}$$

for $i\in\mathcal{I}_0,\ i,j\in\mathcal{I},\ (i,j)\in\Omega$, and

$$\begin{pmatrix}
\boldsymbol{Q}_i & * \\
\boldsymbol{G}_{i(l)} & \boldsymbol{u}_{0(l)}^2/\rho
\end{pmatrix}>0 \text{ for } i\in\mathcal{I},\ l\in\{1,2,\cdots,m\}, \tag{16}$$

where $\boldsymbol{\Theta}_i=\sum_{s=1}^{2^m}\eta_{is}(\boldsymbol{\Lambda}_{is}\boldsymbol{W}_i+\boldsymbol{\Lambda}_{is}^{-}\boldsymbol{G}_i)$, $\overline{\boldsymbol{B}}_i=\sum_{s=1}^{2^m}\eta_{is}\boldsymbol{B}_{1i}\boldsymbol{\Lambda}_{is}$, $\overline{\boldsymbol{D}}_i=\sum_{s=1}^{2^m}\eta_{is}\boldsymbol{D}_{1i}\boldsymbol{\Lambda}_{is}$, $\boldsymbol{W}_i=\boldsymbol{K}_i\boldsymbol{P}_i^{-1}$, $\boldsymbol{G}_i=\boldsymbol{H}_i\boldsymbol{P}_i^{-1}$, and $\boldsymbol{W}_{i(l)}$ and $\boldsymbol{G}_{i(l)}$ denote the l^{th} rows of $\boldsymbol{W}_i$ and $\boldsymbol{G}_i$, respectively, then the closed-loop system (10) is asymptotically stable with H_∞ performance index γ. Moreover, the control parameters in Eq. (4) and Lyapunov matrices in Eq. (14) are given by

$$\boldsymbol{K}_i=\boldsymbol{W}_i\boldsymbol{Q}_i^{-1},\ \ \boldsymbol{P}_i=\boldsymbol{Q}_i^{-1}.$$

Proof Let $\boldsymbol{v}=\boldsymbol{H}_i\boldsymbol{x}$ with $\boldsymbol{H}_i\in\mathbb{R}^{m\times n}$. Based on the piecewise quadratic Lyapunov function (14), it is well known that

$$\begin{aligned}
&\boldsymbol{x}^{\mathrm{T}}(k+1)\boldsymbol{P}_j\boldsymbol{x}(k+1)-\boldsymbol{x}^{\mathrm{T}}(k)\boldsymbol{P}_i\boldsymbol{x}(k)\\
&\quad+\boldsymbol{z}^{\mathrm{T}}(k)\boldsymbol{z}(k)-\gamma^2\boldsymbol{\omega}^{\mathrm{T}}(k)\boldsymbol{\omega}(k)<0
\end{aligned} \tag{17}$$

holds, proving that the closed-loop system (10) is asymptotically stable with H_∞ disturbance attenuation level γ with any $\boldsymbol{\omega}(k)\in l_2[0,\infty)$ (Qiu et al., 2011).

Substituting Eq. (10) into inequality (17) yields

$$\begin{pmatrix}\boldsymbol{x}(k)\\ \boldsymbol{e}(k)\\ \boldsymbol{\omega}(k)\\ 1\end{pmatrix}^{\mathrm{T}}
\begin{pmatrix}
\boldsymbol{A}_i^{\mathrm{T}}\boldsymbol{P}_j\boldsymbol{A}_i-\boldsymbol{P}_i+\overline{\boldsymbol{C}}_i^{\mathrm{T}}\overline{\boldsymbol{C}}_i & * & * \\
\overline{\boldsymbol{B}}_i^{\mathrm{T}}\boldsymbol{P}_j\boldsymbol{A}_i+\boldsymbol{D}_{1i}^{\mathrm{T}}\overline{\boldsymbol{C}}_i & \overline{\boldsymbol{B}}_i^{\mathrm{T}}\boldsymbol{P}_j\overline{\boldsymbol{B}}_i+\boldsymbol{D}_{1i}^{\mathrm{T}}\overline{\boldsymbol{D}}_i & * \\
\boldsymbol{B}_{2i}^{\mathrm{T}}\boldsymbol{P}_j\boldsymbol{A}_i+\boldsymbol{D}_{2i}^{\mathrm{T}}\overline{\boldsymbol{C}}_i & \boldsymbol{B}_{2i}^{\mathrm{T}}\boldsymbol{P}_j\overline{\boldsymbol{B}}_i+\boldsymbol{D}_{2i}^{\mathrm{T}}\overline{\boldsymbol{D}}_i & *\\
\boldsymbol{a}_i^{\mathrm{T}}\boldsymbol{P}_j\boldsymbol{A}_i & \boldsymbol{a}_i^{\mathrm{T}}\boldsymbol{P}_j\overline{\boldsymbol{B}}_i & *\\
\boldsymbol{B}_{2i}^{\mathrm{T}}\boldsymbol{P}_j\boldsymbol{B}_{2i}+\boldsymbol{D}_{2i}^{\mathrm{T}}\boldsymbol{D}_{2i}-\gamma^2\boldsymbol{I} & * \\
\boldsymbol{a}_i^{\mathrm{T}}\boldsymbol{P}_j\boldsymbol{B}_{2i} & \boldsymbol{a}_i^{\mathrm{T}}\boldsymbol{P}_j\boldsymbol{a}_i
\end{pmatrix}
\begin{pmatrix}\boldsymbol{x}(k)\\ \boldsymbol{e}(k)\\ \boldsymbol{\omega}(k)\\ 1\end{pmatrix}<0. \tag{18}$$

From the event-triggering condition (13), we have

$$\boldsymbol{e}^{\mathrm{T}}(k)\boldsymbol{e}(k)<\sigma^2\boldsymbol{x}^{\mathrm{T}}(k)\boldsymbol{K}_i^{\mathrm{T}}\boldsymbol{K}_i\boldsymbol{x}(k), \tag{19}$$

that is,

$$\begin{pmatrix}\boldsymbol{x}(k)\\ \boldsymbol{e}(k)\\ \boldsymbol{\omega}(k)\\ 1\end{pmatrix}^{\mathrm{T}}
\begin{pmatrix}
\sigma^2\boldsymbol{K}_i^{\mathrm{T}}\boldsymbol{K}_i & * & * & * \\
\boldsymbol{0} & -\boldsymbol{I} & * & * \\
\boldsymbol{0} & \boldsymbol{0} & \boldsymbol{0} & * \\
\boldsymbol{0} & \boldsymbol{0} & \boldsymbol{0} & \boldsymbol{0}
\end{pmatrix}
\begin{pmatrix}\boldsymbol{x}(k)\\ \boldsymbol{e}(k)\\ \boldsymbol{\omega}(k)\\ 1\end{pmatrix}>0. \tag{20}$$

Ellipsoid $\boldsymbol{\varepsilon}_i$ (2) can be transformed as

$$\begin{pmatrix}\boldsymbol{x}(k)\\ \boldsymbol{e}(k)\\ \boldsymbol{\omega}(k)\\ 1\end{pmatrix}^{\mathrm{T}}
\begin{pmatrix}
-\boldsymbol{E}_i^{\mathrm{T}}\boldsymbol{E}_i & * & * & * \\
\boldsymbol{0} & \boldsymbol{0} & * & * \\
\boldsymbol{0} & \boldsymbol{0} & \boldsymbol{0} & * \\
-\boldsymbol{f}_i^{\mathrm{T}}\boldsymbol{E}_i & \boldsymbol{0} & \boldsymbol{0} & 1-\boldsymbol{f}_i^{\mathrm{T}}\boldsymbol{f}_i
\end{pmatrix}
\begin{pmatrix}\boldsymbol{x}(k)\\ \boldsymbol{e}(k)\\ \boldsymbol{\omega}(k)\\ 1\end{pmatrix}\geq 0. \tag{21}$$

Applying the S-procedure allows us to combine inequalities (18), (20), and (21) as follows:

$$\begin{pmatrix} \boldsymbol{\Sigma}_1 & * & * \\ -\overline{\boldsymbol{B}}_i^{\mathrm{T}}\boldsymbol{P}_j\overline{\boldsymbol{A}}_i-\overline{\boldsymbol{D}}_i^{\mathrm{T}}\overline{\boldsymbol{C}}_i & \kappa_i\boldsymbol{I}-\overline{\boldsymbol{B}}_i^{\mathrm{T}}\boldsymbol{P}_j\overline{\boldsymbol{B}}_i-\overline{\boldsymbol{D}}_i^{\mathrm{T}}\overline{\boldsymbol{D}}_i & * \\ -\boldsymbol{B}_{2i}^{\mathrm{T}}\boldsymbol{P}_j\overline{\boldsymbol{A}}_i-\boldsymbol{D}_{2i}^{\mathrm{T}}\overline{\boldsymbol{C}}_i & -\boldsymbol{B}_{2i}^{\mathrm{T}}\boldsymbol{P}_j\overline{\boldsymbol{B}}_i-\boldsymbol{D}_{2i}^{\mathrm{T}}\overline{\boldsymbol{D}}_i & * \\ \lambda_i\boldsymbol{f}_i^{\mathrm{T}}\boldsymbol{E}_i-\boldsymbol{a}_i^{\mathrm{T}}\boldsymbol{P}_j\overline{\boldsymbol{A}}_i & -\boldsymbol{a}_i^{\mathrm{T}}\boldsymbol{P}_j\overline{\boldsymbol{B}}_i & \\ & & \gamma^2\boldsymbol{I}-\boldsymbol{B}_{2i}^{\mathrm{T}}\boldsymbol{P}_j\boldsymbol{B}_{2i}-\boldsymbol{D}_{2i}^{\mathrm{T}}\boldsymbol{D}_{2i} \\ & & -\boldsymbol{a}_i^{\mathrm{T}}\boldsymbol{P}_j\boldsymbol{B}_{2i} \end{pmatrix}\begin{matrix} * \\ * \\ * \\ \boldsymbol{\Sigma}_2 \end{matrix}\Bigg) > 0, \quad (22)$$

where $\boldsymbol{\Sigma}_1=\boldsymbol{P}_i-\overline{\boldsymbol{A}}_i^{\mathrm{T}}\boldsymbol{P}_j\overline{\boldsymbol{A}}_i-\overline{\boldsymbol{C}}_i^{\mathrm{T}}\overline{\boldsymbol{C}}_i-\kappa_i\sigma^2\boldsymbol{K}_i^{\mathrm{T}}\boldsymbol{K}_i+\lambda_i\boldsymbol{E}_i^{\mathrm{T}}\boldsymbol{E}_i$ and $\boldsymbol{\Sigma}_2=\lambda_i(\boldsymbol{f}_i^{\mathrm{T}}\boldsymbol{f}_i-1)-\boldsymbol{a}_i^{\mathrm{T}}\boldsymbol{P}_j\boldsymbol{a}_i$.

When the Schur complement is used thrice, the above inequality becomes

$$\begin{pmatrix} \boldsymbol{P}_i+\lambda_i\boldsymbol{E}_i^{\mathrm{T}}\boldsymbol{E}_i & * & * & * & * & * & * \\ \boldsymbol{0} & \kappa_i\boldsymbol{I} & * & * & * & * & * \\ \boldsymbol{0} & \boldsymbol{0} & \gamma^2\boldsymbol{I} & * & * & * & * \\ \lambda_i\boldsymbol{f}_i^{\mathrm{T}}\boldsymbol{E}_i & \boldsymbol{0} & \boldsymbol{0} & \lambda_i(\boldsymbol{f}_i^{\mathrm{T}}\boldsymbol{f}_i-1) & * & * & * \\ \overline{\boldsymbol{A}}_i & \overline{\boldsymbol{B}}_i & \boldsymbol{B}_{2i} & \boldsymbol{a}_i & \boldsymbol{P}_j^{-1} & * & * \\ \overline{\boldsymbol{C}}_i & \overline{\boldsymbol{D}}_i & \boldsymbol{D}_{2i} & \boldsymbol{0} & \boldsymbol{0} & \boldsymbol{I} & * \\ \boldsymbol{K}_i & \boldsymbol{0} & \boldsymbol{0} & \boldsymbol{0} & \boldsymbol{0} & \boldsymbol{0} & \frac{1}{\kappa_i\sigma^2}\boldsymbol{I} \end{pmatrix} > 0. \quad (23)$$

Pre- and post-multiplying inequality (23) by $\mathrm{diag}\left(\boldsymbol{I},\boldsymbol{I},\boldsymbol{I},\begin{pmatrix}\boldsymbol{0},\boldsymbol{0},\boldsymbol{0},\boldsymbol{0}\\ \boldsymbol{0},\boldsymbol{I},\boldsymbol{0},\boldsymbol{0}\\ \boldsymbol{0},\boldsymbol{0},\boldsymbol{I},\boldsymbol{0}\\ \boldsymbol{I},\boldsymbol{0},\boldsymbol{0},\boldsymbol{0}\end{pmatrix}\right)$, its transpose yields

$$\begin{pmatrix} \boldsymbol{P}_i+\lambda_i\boldsymbol{E}_i^{\mathrm{T}}\boldsymbol{E}_i & * & * & * & * & * & * \\ \boldsymbol{0} & \kappa_i\boldsymbol{I} & * & * & * & * & * \\ \boldsymbol{0} & \boldsymbol{0} & \gamma^2\boldsymbol{I} & * & * & * & * \\ \overline{\boldsymbol{A}}_i & \overline{\boldsymbol{B}}_i & \boldsymbol{B}_{2i} & \boldsymbol{P}_j^{-1} & * & * & * \\ \overline{\boldsymbol{C}}_i & \overline{\boldsymbol{D}}_i & \boldsymbol{D}_{2i} & \boldsymbol{0} & \boldsymbol{I} & * & * \\ \boldsymbol{K}_i & \boldsymbol{0} & \boldsymbol{0} & \boldsymbol{0} & \boldsymbol{0} & \frac{1}{\kappa_i\sigma^2}\boldsymbol{I} & * \\ \lambda_i\boldsymbol{f}_i^{\mathrm{T}}\boldsymbol{E}_i & \boldsymbol{0} & \boldsymbol{0} & \boldsymbol{a}_i^{\mathrm{T}} & \boldsymbol{0} & \boldsymbol{0} & \lambda_i(\boldsymbol{f}_i^{\mathrm{T}}\boldsymbol{f}_i-1) \end{pmatrix} > 0. \quad (24)$$

Then, by applying the Schur complement, inequality (24) can be rewritten as

$$\begin{pmatrix} \boldsymbol{P}_i+\lambda_i\boldsymbol{E}_i^{\mathrm{T}}\boldsymbol{E}_i & * & * & * & * & * \\ \boldsymbol{0} & \kappa_i\boldsymbol{I} & * & * & * & * \\ \boldsymbol{0} & \boldsymbol{0} & \gamma^2\boldsymbol{I} & * & * & * \\ \overline{\boldsymbol{A}}_i & \overline{\boldsymbol{B}}_i & \boldsymbol{B}_{2i} & \boldsymbol{P}_j^{-1} & * & * \\ \overline{\boldsymbol{C}}_i & \overline{\boldsymbol{D}}_i & \boldsymbol{D}_{2i} & \boldsymbol{0} & \boldsymbol{I} & * \\ \boldsymbol{K}_i & \boldsymbol{0} & \boldsymbol{0} & \boldsymbol{0} & \boldsymbol{0} & \frac{1}{\kappa_i\sigma^2}\boldsymbol{I} \end{pmatrix} \quad (25)$$
$$-\boldsymbol{\zeta}_1^{\mathrm{T}}\frac{1}{\lambda_i}(\boldsymbol{f}_i^{\mathrm{T}}\boldsymbol{f}_i-1)^{-1}\boldsymbol{\zeta}_1>0,$$

where $\boldsymbol{\zeta}_1=\begin{pmatrix}\lambda_i\boldsymbol{f}_i^{\mathrm{T}}\boldsymbol{E}_i & \boldsymbol{0} & \boldsymbol{0} & \boldsymbol{a}_i^{\mathrm{T}} & \boldsymbol{0} & \boldsymbol{0}\end{pmatrix}$.

According to the inversion lemma $(\boldsymbol{A}+\boldsymbol{BCD})^{-1}=\boldsymbol{A}^{-1}-\boldsymbol{A}^{-1}\boldsymbol{B}(\boldsymbol{C}^{-1}+\boldsymbol{DA}^{-1}\boldsymbol{B})^{-1}\boldsymbol{DA}^{-1}$ (Kailath, 1980), we have

$$\begin{cases} (\boldsymbol{I}-\boldsymbol{f}_i^{\mathrm{T}}\boldsymbol{f}_i)^{-1}=\boldsymbol{I}+\boldsymbol{f}_i^{\mathrm{T}}(\boldsymbol{I}-\boldsymbol{f}_i\boldsymbol{f}_i^{\mathrm{T}})^{-1}\boldsymbol{f}_i, \\ \boldsymbol{f}_i(\boldsymbol{I}-\boldsymbol{f}_i^{\mathrm{T}}\boldsymbol{f}_i)^{-1}=(\boldsymbol{I}-\boldsymbol{f}_i\boldsymbol{f}_i^{\mathrm{T}})^{-1}\boldsymbol{f}_i. \end{cases} \quad (26)$$

Through simple calculation, inequality (25) becomes

$$\begin{pmatrix} \boldsymbol{P}_i & * & * & * & * & * \\ \boldsymbol{0} & \kappa_i\boldsymbol{I} & * & * & * & * \\ \boldsymbol{0} & \boldsymbol{0} & \gamma^2\boldsymbol{I} & * & * & * \\ \overline{\boldsymbol{A}}_i & \overline{\boldsymbol{B}}_i & \boldsymbol{B}_{2i} & \boldsymbol{P}_j^{-1}+\frac{1}{\lambda_i}\boldsymbol{a}_i\boldsymbol{a}_i^{\mathrm{T}} & * & * \\ \overline{\boldsymbol{C}}_i & \overline{\boldsymbol{D}}_i & \boldsymbol{D}_{2i} & \boldsymbol{0} & \boldsymbol{I} & * \\ \boldsymbol{K}_i & \boldsymbol{0} & \boldsymbol{0} & \boldsymbol{0} & \boldsymbol{0} & \frac{1}{\kappa_i\sigma^2}\boldsymbol{I} \end{pmatrix} \quad (27)$$
$$-\boldsymbol{\zeta}_2^{\mathrm{T}}\lambda_i(\boldsymbol{f}_i\boldsymbol{f}_i^{\mathrm{T}}-\boldsymbol{I})^{-1}\boldsymbol{\zeta}_2>0,$$

where $\boldsymbol{\zeta}_2=\begin{pmatrix}\boldsymbol{E}_i & \boldsymbol{0} & \boldsymbol{0} & \frac{1}{\lambda_i}\boldsymbol{f}_i^{\mathrm{T}}\boldsymbol{a}_i & \boldsymbol{0} & \boldsymbol{0}\end{pmatrix}$.

Now, by applying the Schur complement again, inequality (27) becomes

$$\begin{pmatrix} \boldsymbol{P}_i & * & * & * & * & * & * \\ \boldsymbol{0} & \kappa_i\boldsymbol{I} & * & * & * & * & * \\ \boldsymbol{0} & \boldsymbol{0} & \gamma^2\boldsymbol{I} & * & * & * & * \\ \overline{\boldsymbol{A}}_i & \overline{\boldsymbol{B}}_i & \boldsymbol{B}_{2i} & \boldsymbol{P}_j^{-1}+\frac{1}{\lambda_i}\boldsymbol{a}_i\boldsymbol{a}_i^{\mathrm{T}} & * & * & * \\ \overline{\boldsymbol{C}}_i & \overline{\boldsymbol{D}}_i & \boldsymbol{D}_{2i} & \boldsymbol{0} & \boldsymbol{I} & * & * \\ \boldsymbol{K}_i & \boldsymbol{0} & \boldsymbol{0} & \boldsymbol{0} & \boldsymbol{0} & \frac{1}{\kappa_i\sigma^2}\boldsymbol{I} & * \\ \boldsymbol{E}_i & \boldsymbol{0} & \boldsymbol{0} & \frac{1}{\lambda_i}\boldsymbol{f}_i\boldsymbol{a}_i^{\mathrm{T}} & \boldsymbol{0} & \boldsymbol{0} & \frac{1}{\lambda_i}(\boldsymbol{f}_i\boldsymbol{f}_i^{\mathrm{T}}-\boldsymbol{I}) \end{pmatrix} > 0. \quad (28)$$

Pre- and post-multiplying inequality (28) by $\mathrm{diag}(\boldsymbol{P}_i^{-1},\frac{1}{\kappa_i}\boldsymbol{I},\boldsymbol{I},\boldsymbol{I},\boldsymbol{I},\boldsymbol{I},\boldsymbol{I})$, we obtain

$$\begin{pmatrix} \boldsymbol{P}_i^{-1} & * & * & * & * & * & * \\ \boldsymbol{0} & \frac{1}{\kappa_i}\boldsymbol{I} & * & * & * & * & * \\ \boldsymbol{0} & \boldsymbol{0} & \gamma^2\boldsymbol{I} & * & * & * & * \\ \overline{\boldsymbol{A}}_i\boldsymbol{P}_i^{-1} & \frac{1}{\kappa_i}\overline{\boldsymbol{B}}_i & \boldsymbol{B}_{2i} & \boldsymbol{P}_j^{-1}+\frac{1}{\lambda_i}\boldsymbol{a}_i\boldsymbol{a}_i^{\mathrm{T}} & * & * & * \\ \overline{\boldsymbol{C}}_i\boldsymbol{P}_i^{-1} & \frac{1}{\kappa_i}\overline{\boldsymbol{D}}_i & \boldsymbol{D}_{2i} & \boldsymbol{0} & \boldsymbol{I} & * & * \\ \boldsymbol{K}_i\boldsymbol{P}_i^{-1} & \boldsymbol{0} & \boldsymbol{0} & \boldsymbol{0} & \boldsymbol{0} & \frac{1}{\kappa_i\sigma^2}\boldsymbol{I} & * \\ \boldsymbol{E}_i\boldsymbol{P}_i^{-1} & \boldsymbol{0} & \boldsymbol{0} & \frac{1}{\lambda_i}\boldsymbol{f}_i\boldsymbol{a}_i^{\mathrm{T}} & \boldsymbol{0} & \boldsymbol{0} & \frac{1}{\lambda_i}(\boldsymbol{f}_i\boldsymbol{f}_i^{\mathrm{T}}-\boldsymbol{I}) \end{pmatrix} > 0. \quad (29)$$

Thus, inequality (29) is transformed to inequality (15a) by $\boldsymbol{Q}_i=\boldsymbol{P}_i^{-1}$, $\boldsymbol{W}_i=\boldsymbol{K}_i\boldsymbol{Q}_i$, $\boldsymbol{G}_i=\boldsymbol{H}_i\boldsymbol{Q}_i$, $\alpha_i=\frac{1}{\kappa_i}$, and $\beta_i=\frac{1}{\lambda_i}$. For $i\in\mathcal{I}_0$, the subsystem is treated as a linear system, and through similar derivation, the LMI can be written as inequality (15b).

By performing pre- and post-multiplication for inequality (8) by $\mathrm{diag}\begin{pmatrix}\boldsymbol{P}_i^{-1} & \boldsymbol{I}\end{pmatrix}$, LMI (16) can be obtained by substituting $\boldsymbol{Q}_i=\boldsymbol{P}_i^{-1}$ and $\boldsymbol{G}_{i(l)}=\boldsymbol{H}_{i(l)}\boldsymbol{P}_i^{-1}$. Hence, it can be concluded that LMI (16) ensures $\xi(\boldsymbol{P}_i,\rho)\subset\mathscr{L}(\boldsymbol{H}_i,\boldsymbol{u}_0)$. This completes the proof.

Remark 3 When $\boldsymbol{f}_i^{\mathrm{T}}\boldsymbol{f}_i-1\le 0$, inequality (15) has no feasible solution; then, the subsystem lies inside ellipsoid $\boldsymbol{\varepsilon}_i$. In this case, ΔV is negative for $\boldsymbol{x}(k)\in\boldsymbol{\varepsilon}_i$ if $\boldsymbol{A}_i^{\mathrm{T}}\boldsymbol{P}_j\boldsymbol{A}_i-\boldsymbol{P}_i<0$, which is equivalent to inequality (15b).

Remark 4 For the design of event-triggered controllers of the PWA systems in Ma et al. (2018, 2019), the nonlinear term $\gamma_i\boldsymbol{Q}_i\overline{\boldsymbol{E}}_i\boldsymbol{Q}_i$ was relaxed according to $\gamma_i\boldsymbol{Q}_i\overline{\boldsymbol{E}}_i\boldsymbol{Q}_i\ge\boldsymbol{Q}_i\overline{\boldsymbol{E}}_i^{\frac{1}{2}}+\overline{\boldsymbol{E}}_i^{\frac{1}{2}}\boldsymbol{Q}_i-\gamma_i^{-1}\boldsymbol{I}$. This

method resulted in conservativeness to some extent. In this study, the inversion lemma is applied to deal with the term $\lambda_i \boldsymbol{E}_i^{\mathrm{T}} \boldsymbol{E}_i$ in inequality (25), thereby avoiding the conservativeness in handling the nonlinear term in LMI.

Remark 5 By introducing constraint $\boldsymbol{P}_i = \boldsymbol{P}$, the piecewise quadratic Lyapunov function (14) becomes a common quadratic Lyapunov function (Rodrigues and Boyd, 2005; LeBel and Rodrigues, 2009). Obviously, the common Lyapunov function is more conservative than the piecewise Lyapunov function.

The smallest H_∞ performance index can be measured by solving the following optimization problem:

Optimization problem 1:

$$\begin{aligned} &\min_{\boldsymbol{W}_i,\, \boldsymbol{Q}_i} \quad \gamma, \ \ i \in \mathcal{I}, \\ &\text{subject to inequalities (15) and (16).} \end{aligned} \tag{30}$$

For a fixed γ, the region of attraction can be maximized by the following optimization problem:

Optimization problem 2:

$$\begin{aligned} &\min_{\boldsymbol{W}_i,\, \boldsymbol{Q}_i} \quad \mathrm{tr}(\boldsymbol{Q}_i^{-1}), \ \ i \in \mathcal{I}, \\ &\text{subject to inequalities (15) and (16).} \end{aligned} \tag{31}$$

Remark 6 As the optimization goals of optimization problems 1 and 2 are convex functions (Boyd and Vandenberghe, 2004), LMIs in Theorem 1 can be numerically effectively solved in MATLAB using toolbox CVX (Grant and Boyd, 2014) as an interface and SDPT3 (Toh et al., 1999)/SeDuMi (Sturm, 1999) as a solver.

Remark 7 When using PWA systems to approximate nonlinear systems, more subsystems are needed if a higher accuracy is required. In such a situation, one should be aware of the fundamental limitations of computations. For each subsystem, the number of free variables in Theorem 1 is $N = \frac{1}{2}n^2 + \frac{1}{2}n + 2mn + 3$. In contrast, the number of free variables in Theorem 1 in Ma et al. (2019) was $N = \frac{1}{2}n^2 + \frac{1}{2}n + 2mn + 3m + 2$, which is larger. Note that robustness was not discussed in Ma et al. (2019). Consequently, our method has lower complexity.

4 Examples

In this section, we present a discrete-time chaotic map-T system and a single-link robot arm control system to demonstrate the merits and effectiveness of the proposed controller design method. Comparisons are made with methods in the literature. The transmission reduction is measured by the control input update rate or, equivalently, the transmission rate (TR), which is defined as follows:

$$\mathrm{TR} = \frac{\text{Number of event triggers}}{\text{Number of measurements}}.$$

Example 1 Consider the following discrete-time chaotic map-T system (Chen CL et al., 2005) with modifications:

$$\boldsymbol{x}(k+1) = \begin{cases} \boldsymbol{A}_1\boldsymbol{x}(k) + \boldsymbol{B}_{11}\boldsymbol{u}(k) + \boldsymbol{B}_{21}\boldsymbol{\omega}(k) + \boldsymbol{a}_1, \\ \quad -10 \le x_1 < 6, \\ \boldsymbol{A}_2\boldsymbol{x}(k) + \boldsymbol{B}_{12}\boldsymbol{u}(k) + \boldsymbol{B}_{22}\boldsymbol{\omega}(k) + \boldsymbol{a}_2, \\ \quad 6 \le x_1 \le 10, \end{cases}$$

$$\boldsymbol{z}(k) = \boldsymbol{C}\boldsymbol{x}(k) + \boldsymbol{D}\boldsymbol{u}(k),$$

with

$$\boldsymbol{A}_i = \begin{pmatrix} 0 & 0.89 & 0.5 \\ h_i & 0.89 & 0 \\ -0.1 & 0 & 0.9 \end{pmatrix}, \ \ \boldsymbol{a}_1 = \begin{pmatrix} 0 \\ 0 \\ 0 \end{pmatrix},$$

$$\boldsymbol{a}_2 = \begin{pmatrix} 0 \\ -18.72 \\ 0 \end{pmatrix}, \ \boldsymbol{B}_{11} = \begin{pmatrix} 1 \\ 0 \\ 1.5 \end{pmatrix}, \ \boldsymbol{B}_{12} = \begin{pmatrix} 0.5 \\ 0 \\ 0 \end{pmatrix},$$

$$\boldsymbol{B}_{21} = \boldsymbol{B}_{22} = \begin{pmatrix} 0.01 \\ 0.01 \\ 0.01 \end{pmatrix}, \ \boldsymbol{C} = \begin{pmatrix} 0.5 & 0.5 & 0.5 \end{pmatrix},$$

$$\boldsymbol{D} = (0.1), \ i = 1, 2, \ h_1 = -1.12, \ h_2 = 2.$$

The state spaces of these two subsystems can be described by the degenerate ellipsoid (2) with $\boldsymbol{E}_1 = \begin{pmatrix} 0.125 & 0 & 0 \end{pmatrix}$, $\boldsymbol{f}_1 = (0.25)$, $\boldsymbol{E}_2 = \begin{pmatrix} 0.5 & 0 & 0 \end{pmatrix}$, and $\boldsymbol{f}_2 = (-4)$.

Let $\sigma = 0.9$. By solving Theorem 1, we can obtain the controller gains as

$$\begin{cases} \boldsymbol{K}_1 = (0.3158 \ \ -0.8499 \ \ -0.5128), \\ \boldsymbol{K}_2 = (0.3661 \ \ -0.5736 \ \ -0.3334). \end{cases}$$

For comparison, we obtain the following controller gains by applying Theorem 3 in Chen YG et al. (2014):

$$\begin{cases} \boldsymbol{K}_1 = (0.5158 \ \ -0.7569 \ \ -0.5576), \\ \boldsymbol{K}_2 = (0.5722 \ \ -1.2075 \ \ -0.8641). \end{cases}$$

The initial condition is taken as $\boldsymbol{x}(0) = \begin{pmatrix} 10 & -0.4 & 1 \end{pmatrix}^{\mathrm{T}}$ in $\boldsymbol{\chi}_2$, and the number of sampling steps is set to 50. For an external disturbance

$\omega(k) = 50\exp(-0.2t)\sin(2\pi t)$, the results obtained by our approach and those based on Chen YG et al. (2014)'s approach are shown in Figs. 2–4 for comparison. Fig. 2 shows the state responses of the system. It can be seen that the system converges faster when our approach is used. The control inputs are shown in Fig. 3. Event triggers are recorded in Fig. 4, where "1" means that the event is triggered, and "0" means that it is not. Fig. 4 shows that events occur at every event sampling instant when Chen YG et al. (2014)'s approach is adopted; in contrast, events are significantly reduced when our approach is used, implying that communication resources can be greatly conserved using our approach. Table 1 lists the TR and the minimum H_∞ performance index $\gamma_{\min}$ for different values of σ when solving the optimization problem 1.

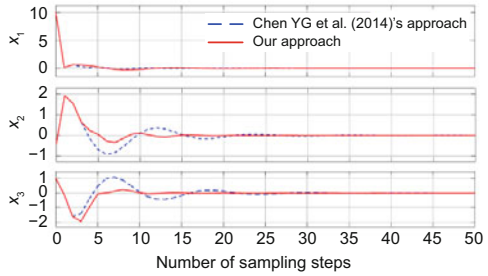


Fig. 2 State responses of the system when $\sigma = 0.9$

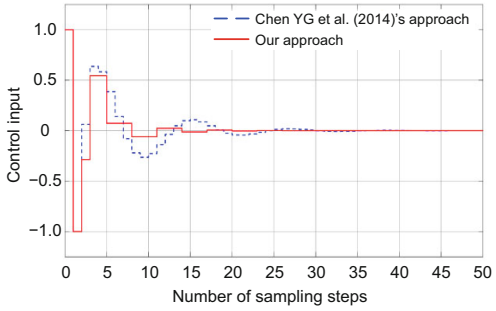


Fig. 3 Control input of the system when $\sigma = 0.9$

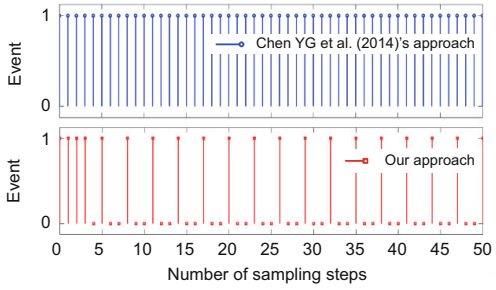


Fig. 4 Simulation results of the events when $\sigma = 0.9$
"1" means that the event is triggered and "0" means that it is not triggered

Table 1 shows that the larger the event-triggering threshold σ, the fewer the events triggered. However, H_∞ performance worsens with a higher threshold. Consequently, a trade-off between TR and the H_∞ performance is necessary. For specific situations, a proper control performance and an appropriate TR can be obtained by adjusting the value of σ.

Table 1 H_∞ performance index $\gamma_{\min}$ and transmission rate (TR) for various values of σ

σ	$\gamma_{\min}$	TR (%)
0.1	0.0406	94.12
0.3	0.0795	74.51
0.5	0.2616	66.67
0.7	6.0865	52.94
0.9	11.7065	39.22

Example 2 Consider the following single-link robot arm control system (Zhang et al., 2017):

$$\ddot{\theta}(t) = -\frac{MgL}{J}\sin(\theta(t)) - \frac{R}{J}\dot{\theta}(t) + \frac{1}{J}u(t) + \omega(t),$$

where $\theta(t)$ is the angle of the arm, $u(t)$ the control input, $\omega(t)$ the external disturbance, M the mass of the payload, J the moment of inertia, g the acceleration of gravity, L the length of the arm, and R the coefficient of the viscous friction. Parameters are selected as follows: $M = 1$ kg, $J = 1$ kg $\cdot$ m^2, $g = 9.8$ m/s^2, $L = 1$ m, $R = 0.5$ kg $\cdot$ m/s^2.

By defining $x_1(t) = \theta(t)$, $x_2(t) = \dot{\theta}(t)$, $\boldsymbol{x}(t) = (x_1(t)\ x_2(t))^{\mathrm{T}}$, and $z(t) = x_1(t) + 0.3\omega(t)$, the system can be expressed as follows:

$$\begin{cases} \dot{x}_1(t) = x_2(t), \\ \dot{x}_2(t) = -9.8\sin(x_1(t)) - 0.5x_2(t) + u(t) + \omega(t), \\ z(t) = x_1(t) + 0.3\omega(t). \end{cases}$$

The characteristic of the nonlinear term $\sin x_1$ is approximated by a piecewise function. An illustration of the approximation effect is given in Fig. 5. The state space is partitioned into three regions:

$$\begin{cases} \boldsymbol{\chi}_1 = \left\{\boldsymbol{x} \in \mathbb{R}^2 | -\dfrac{3\pi}{5} \le x_1 < -\dfrac{\pi}{5}\right\}, \\ \boldsymbol{\chi}_2 = \left\{\boldsymbol{x} \in \mathbb{R}^2 | -\dfrac{\pi}{5} \le x_1 < \dfrac{\pi}{5}\right\}, \\ \boldsymbol{\chi}_3 = \left\{\boldsymbol{x} \in \mathbb{R}^2 | \dfrac{\pi}{5} \le x_1 \le \dfrac{3\pi}{5}\right\}. \end{cases}$$

By discretizing the system with period $T = 0.1$ s, we end up with the discrete-time PWA

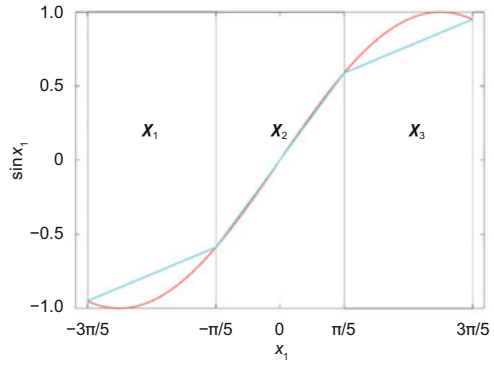


Fig. 5 Piecewise affine (PWA) approximation of $\sin x_1$

model (1) with

$$\boldsymbol{A}_1=\boldsymbol{A}_3=\begin{pmatrix}0.9861 & 0.0971\\ -0.2750 & 0.9376\end{pmatrix},\ \boldsymbol{a}_2=\begin{pmatrix}0\\0\end{pmatrix},$$

$$\boldsymbol{A}_2=\begin{pmatrix}0.9553 & 0.0961\\ -0.8806 & 0.9072\end{pmatrix},\boldsymbol{a}_1=-\boldsymbol{a}_3=\begin{pmatrix}0.0195\\0.3864\end{pmatrix},$$

$$\boldsymbol{B}_{11}=\boldsymbol{B}_{13}=\boldsymbol{B}_{21}=\boldsymbol{B}_{23}=\begin{pmatrix}0.0049\\0.0971\end{pmatrix},$$

$$\boldsymbol{B}_{12}=\boldsymbol{B}_{22}=\begin{pmatrix}0.0049\\0.0961\end{pmatrix},\ \boldsymbol{C}_1=\boldsymbol{C}_2=\boldsymbol{C}_3=\begin{pmatrix}1 & 0\end{pmatrix},$$

$$\boldsymbol{D}_{11}=\boldsymbol{D}_{12}=\boldsymbol{D}_{13}=(0),\ \boldsymbol{D}_{21}=\boldsymbol{D}_{22}=\boldsymbol{D}_{23}=(0.3).$$

Here, using degenerate ellipsoid (2) to (exactly) cover the polytopic regions, we obtain $\boldsymbol{E}_1=\boldsymbol{E}_2=\boldsymbol{E}_3=\begin{pmatrix}\frac{5}{\pi} & 0\end{pmatrix}$, $\boldsymbol{f}_1=-\boldsymbol{f}_3=(2)$, and $\boldsymbol{f}_2=(0)$.

For the above saturated PWA system, we are interested in designing an event-triggered controller (5) such that the closed-loop system (10) is asymptotically stable with a guaranteed H_∞ disturbance attenuation level $\gamma_{\min}$ while the signal transmission is reduced. Considering $\boldsymbol{u}_0=(1)$, $\sigma=0.7$, and $\gamma=1$ for the optimization problem 2, the controller gains and Lyapunov matrices are obtained as follows:

$$\boldsymbol{K}_1=\boldsymbol{K}_3=\begin{pmatrix}-53.3438 & -11.9312\end{pmatrix},$$

$$\boldsymbol{K}_2=\begin{pmatrix}-48.2323 & -11.7772\end{pmatrix},$$

$$\boldsymbol{P}_1=\boldsymbol{P}_3=\begin{pmatrix}3.4593 & 0.3213\\ 0.3213 & 0.0924\end{pmatrix},$$

$$\boldsymbol{P}_2=\begin{pmatrix}3.4092 & 0.3135\\ 0.3135 & 0.0904\end{pmatrix}.$$

To simulate the performance of the derived controller, two cases are considered:

Case 1 (Without disturbance) Consider an undisturbed system, i.e., $\omega(t)=0$.

Case 2 (With disturbance) Assume that the system is subject to an external disturbance $\omega(t)=0.5\sin(4\pi t)$.

Applying the controller given above, the simulation results are shown in Figs. 6–9 with initial condition $\boldsymbol{x}_0=\begin{pmatrix}0.23\pi & -0.13\pi\end{pmatrix}^{\mathrm{T}}$ and simulation time $t=10$ s. Fig. 6 depicts the state responses of the system without disturbance. It is seen that the closed-loop stability is ensured using the proposed controller. Fig. 7 shows the control input without disturbance. Figs. 8 and 9 show the state responses and control input of the system with disturbance, respectively. From Fig. 8, it is seen that the state of the system is maintained near the origin.

The estimate of the domain of attraction when $\sigma=0.7$ is shown in Fig. 10. The domain of attraction can be significantly enlarged for the optimization problem 2. For different values of σ, the estimate of the domain of attraction is shown in Fig. 11. It is clear that with increasing σ, the estimate of the domain of attraction decreases. Table 2 presents the comparison of TR between a previous approach (Wu et al., 2014; Ma et al., 2019) and the proposed Algorithm 1 with different values of σ.

Table 2 Comparison of the transmission rate (TR) with various values of σ

σ	TR (%)			
	Strategy in Wu et al. (2014) and Ma et al. (2019)		Algorithm 1	
	Case 1	Case 2	Case 1	Case 2
0.01	99.01	100	47.52	48.51
0.1	90.10	85.15	47.52	42.57
0.3	78.22	67.33	52.48	45.54
0.7	52.48	48.51	48.51	43.56
0.9	21.78	24.75	20.79	24.75

Table 2 shows that for the triggering technique in Wu et al. (2014) and Ma et al. (2019), the larger the event-triggering threshold σ, the fewer the events triggered. In addition, Table 2 and Fig. 11 indicate that there exists a trade-off between TR and the control performance. However, because of actuator saturation, resources may be wasted. Obviously, by applying Algorithm 1, TR can be further reduced. In fact, TR may be affected by parameter uncertainties, disturbances, and actuator saturations. In practical applications, appropriate control performance can be obtained by adjusting the value of σ.

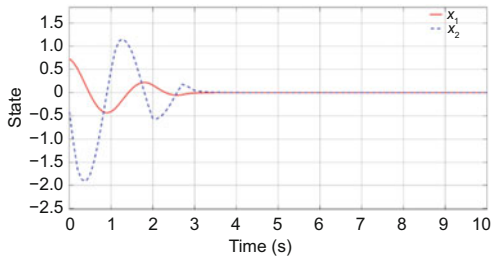


Fig. 6 State response of the system in case 1 when $\sigma = 0.7$

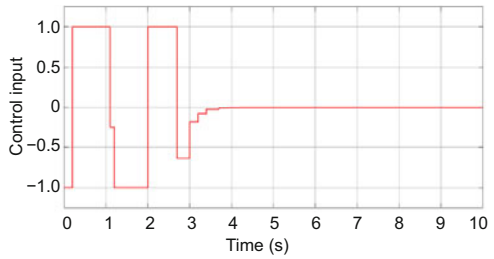


Fig. 7 Control input of the system in case 1 when $\sigma = 0.7$

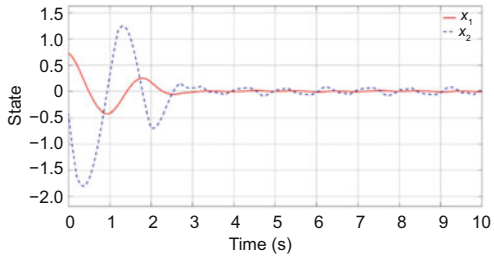


Fig. 8 State response of the system in case 2 when $\sigma = 0.7$

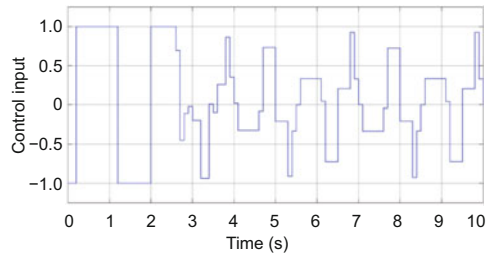


Fig. 9 Control input of the system in case 2 when $\sigma = 0.7$

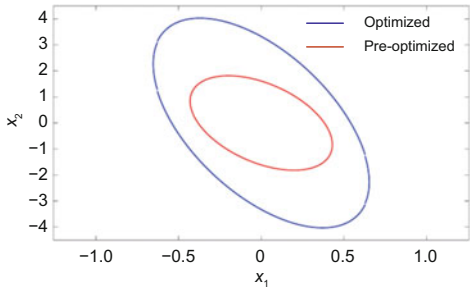


Fig. 10 Estimate of the domain of attraction when $\sigma = 0.7$

References to color refer to the online version of this figure

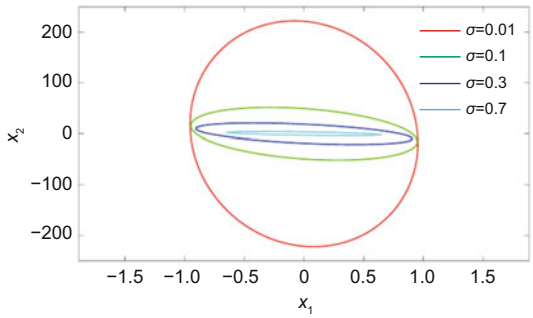


Fig. 11 Estimate of the domain of attraction with different values of σ

References to color refer to the online version of this figure

5 Conclusions

We have studied the event-triggered H_∞ control for discrete-time PWA systems subject to actuator saturation. A novel event-triggered strategy that considers the saturation information has been proposed. With the aid of a piecewise Lyapunov function combined with S-procedure and some matrix linearization procedures, sufficient conditions for novel event-triggered H_∞ controllers have been formulated as LMIs that can be efficiently solved by available software. Numerical examples have been provided to confirm the effectiveness of the proposed approach.

Contributors

Yonghao JIANG and Wei WU designed the research. Yonghao JIANG performed the simulation and drafted the manuscript. Wei WU, Xuyang LOU, and Zhengxian JIANG helped organize the manuscript. Wei WU, Xuyang LOU, and Baotong CUI revised and finalized the paper.

Compliance with ethics guidelines

Yonghao JIANG, Wei WU, Xuyang LOU, Zhengxian JIANG, and Baotong CUI declare that they have no conflict of interest.

References

Åarzén KE, 1999. A simple event-based PID controller. *IFAC Proc Vol*, 32(2):8687-8692. https://doi.org/10.1016/s1474-6670(17)57482-0

Aranda-Escolástico E, Abdelrahim M, Guinaldo M, et al., 2017. Design of periodic event-triggered control for polynomial systems: a delay system approach. *IFAC-PapersOnLine*, 50(1):7887-7892. https://doi.org/10.1016/j.ifacol.2017.08.748

Åström KJ, Bernhardsson B, 1999. Comparison of periodic and event based sampling for first-order stochastic systems. *IFAC Proc Vol*, 32(2):5006-5011. https://doi.org/10.1016/s1474-6670(17)56852-4

Boyd S, Vandenberghe L, 2004. Convex Optimization. Cambridge University Press, Cambridge, UK.

Chen CL, Feng G, Guan XP, 2005. H_∞ discrete time fuzzy control with application to chaos control based on piecewise Lyapunov functions. *IFAC Proc Vol*, 38(1):449-454. https://doi.org/10.3182/20050703-6-cz-1902.01153

Chen YG, Zhou Q, Fei SM, 2014. Robust stabilization and l_2-gain control of uncertain discrete-time constrained piecewise-affine systems. *Nonl Dynam*, 75(1-2):127-140. https://doi.org/10.1007/s11071-013-1054-x

Eqtami A, Dimarogonas DV, Kyriakopoulos KJ, 2010. Event-triggered control for discrete-time systems. Proc American Control Conf, p.4719-4724. https://doi.org/10.1109/acc.2010.5531089

Esfahani PS, Pieper JK, 2017. H_∞ model predictive control for constrained discrete-time piecewise affine systems. *Int J Rob Nonl Contr*, 28(6):1973-1995. https://doi.org/10.1002/rnc.3995

Gao Y, Liu Z, Chen H, 2009. Robust H_∞ control for constrained discrete-time piecewise affine systems with time-varying parametric uncertainties. *IET Contr Theory Appl*, 3(8):1132-1144. https://doi.org/10.1049/iet-cta.2008.0182

Grant M, Boyd S, 2014. CVX: Matlab Software for Disciplined Convex Programming. Version 2.2. http://cvxr.com/cvx

Heemels WPMH, de Schutter B, Bemporad A, 2001. Equivalence of hybrid dynamical models. *Automatica*, 37(7):1085-1091. https://doi.org/10.1016/s0005-1098(01)00059-0

Heemels WPMH, Donkers MCF, Teel AR, 2013. Periodic event-triggered control for linear systems. *IEEE Trans Autom Contr*, 58(4):847-861. https://doi.org/10.1109/tac.2012.2220443

Hespanha JP, Naghshtabrizi P, Xu YG, 2007. A survey of recent results in networked control systems. *Proc IEEE*, 95(1):138-162. https://doi.org/10.1109/jproc.2006.887288

Hu TS, Lin ZL, Chen BM, 2002. Analysis and design for discrete-time linear systems subject to actuator saturation. *Syst Contr Lett*, 45(2):97-112. https://doi.org/10.1016/s0167-6911(01)00168-2

Kailath T, 1980. Linear Systems. Prentice-Hall, Englewood Cliffs, USA.

LeBel S, Rodrigues L, 2009. PWL and PWA H_∞ controller synthesis for uncertain PWA slab systems: LMI approach. *Int J Contr*, 82(3):482-492. https://doi.org/10.1080/00207170802144313

Lei Y, Wang YW, Guan ZH, et al., 2018. Event-triggered adaptive output regulation for a class of nonlinear systems with unknown control direction. *IEEE Trans Syst Man Cybern Syst*, in press. https://doi.org/10.1109/tsmc.2018.2852700

Li HC, Zuo ZQ, Wang YJ, 2018. Dynamic output feedback control for systems subject to actuator saturation via event-triggered scheme. *Asian J Contr*, 20(1):207-215. https://doi.org/10.1002/asjc.1662

Liu JL, Yin TT, Yue D, et al., 2020a. Event-based secure leader-following consensus control for multiagent systems with multiple cyber attacks. *IEEE Trans Cybern*, in press. https://doi.org/10.1109/tcyb.2020.2970556

Liu JL, Yang M, Xie XP, et al., 2020b. Finite-time H_∞ filtering for state-dependent uncertain systems with event-triggered mechanism and multiple attacks. *IEEE Trans Circ Syst I*, 67(3):1021-1034. https://doi.org/10.1109/tcsi.2019.2949014

Liu JL, Suo W, Zha LJ, et al., 2020c. Security distributed state estimation for nonlinear networked systems against DoS attacks. *Int J Rob Nonl Contr*, 30(3):1156-1180. https://doi.org/10.1002/rnc.4815

Liu Y, Yang GH, Li XJ, 2017. Event-triggered fault detection observer design for affine fuzzy systems. *Neurocomputing*, 267:564-571. https://doi.org/10.1016/j.neucom.2017.06.033

Ma YF, Wu W, Cui BT, 2018. Event-triggered feedback control for discrete-time piecewise-affine systems. *Int J Syst Sci*, 49(16):3377-3389. https://doi.org/10.1080/00207721.2018.1541262

Ma YF, Wu W, Görges D, et al., 2019. Event-triggered feedback control for discrete-time piecewise affine systems subject to input saturation. *Nonl Dynam*, 95(3):2353-2365. https://doi.org/10.1007/s11071-018-4696-x

Postoyan R, Tabuada P, Nešić D, et al., 2015. A framework for the event-triggered stabilization of nonlinear systems. *IEEE Trans Autom Contr*, 60(4):982-996. https://doi.org/10.1109/tac.2014.2363603

Qiu JB, Feng G, Gao HJ, 2011. Approaches to robust H_∞ static output feedback control of discrete-time piecewise-affine systems with norm-bounded uncertainties. *Int J Rob Nonl Contr*, 21(7):790-814. https://doi.org/10.1002/rnc.1627

Qiu JB, Wei YL, Wu LG, 2017. A novel approach to reliable control of piecewise affine systems with actuator faults. *IEEE Trans Circ Syst II*, 64(8):957-961. https://doi.org/10.1109/tcsii.2016.2629663

Qiu JB, Wei YL, Karimi HR, et al., 2018. Reliable control of discrete-time piecewise-affine time-delay systems via output feedback. *IEEE Trans Reliab*, 67(1):79-91. https://doi.org/10.1109/tr.2017.2749242

Rodrigues L, Boukas EK, 2006. Piecewise-linear H_∞ controller synthesis with applications to inventory control of switched production systems. *Automatica*, 42(8):1245-1254. https://doi.org/10.1016/j.automatica.2006.04.004

Rodrigues L, Boyd S, 2005. Piecewise-affine state feedback for piecewise-affine slab systems using convex optimization. *Syst Contr Lett*, 54(9):835-853. https://doi.org/10.1016/j.sysconle.2005.01.002

Saito T, Jinąźno K, Torikai H, 1995. Chaotic artificial neural system and its control. *Int J Electron*, 79(6):797-806. https://doi.org/10.1080/00207219508926313

Sontag E, 1981. Nonlinear regulation: the piecewise linear approach. *IEEE Trans Autom Contr*, 26(2):346-358. https://doi.org/10.1109/tac.1981.1102596

Sturm JF, 1999. Using SeDuMi 1.02, a Matlab toolbox for optimization over symmetric cones. *Optim Method Softw*, 11(1-4):625-653. https://doi.org/10.1080/10556789908805766

Tabuada P, 2007. Event-triggered real-time scheduling of stabilizing control tasks. *IEEE Trans Autom Contr*, 52(9):1680-1685. https://doi.org/10.1109/tac.2007.904277

Tarbouriech S, Garcia G, da Silva JMGJr, et al., 2011. Stability and Stabilization of Linear Systems with Saturating Actuators. Springer, London, UK. https://doi.org/10.1007/978-0-85729-941-3

Toh KC, Todd MJ, Tütüncü RH, 1999. SDPT3—a Matlab software package for semidefinite programming. Version 1.3. *Optim Method Softw*, 11(1-4):545-581. https://doi.org/10.1080/10556789908805762

Wu W, Reimann S, Liu S, 2014. Event-triggered control for linear systems subject to actuator saturation. *IFAC Proc Vol*, 47(3):9492-9497. https://doi.org/10.3182/20140824-6-za-1003.00255

Wu W, Reimann S, Görges D, et al., 2015. Suboptimal event-triggered control for time-delayed linear systems. *IEEE Trans Autom Contr*, 60(5):1386-1391. https://doi.org/10.1109/tac.2014.2347214

Wu W, Reimann S, Görges D, et al., 2016. Event-triggered control for discrete-time linear systems subject to bounded disturbance. *Int J Rob Nonl Contr*, 26(9):1902-1918. https://doi.org/10.1002/rnc.3388

Zhang LX, Ning ZP, Zhang WX, 2017. Observer-based control for piecewise-affine systems with both input and output quantization. *IEEE Trans Autom Contr*, 62(11):5858-5865. https://doi.org/10.1109/tac.2016.2641585

Zuo ZQ, Li QS, Li HC, et al., 2016. Co-design of event-triggered control for discrete-time systems with actuator saturation. Proc 12th World Congress on Intelligent Control and Automation, p.170-175. https://doi.org/10.1109/wcica.2016.7578438